A Microtubule-associated Protein from *Xenopus* Eggs That Specifically Promotes Assembly at the Plus-End

David L. Gard and Marc W. Kirschner

Department of Biochemistry and Biophysics, University of California School of Medicine, San Francisco, California 94143

Abstract. We have isolated a protein factor from *Xenopus* eggs that promotes microtubule assembly in vitro. Assembly promotion was associated with a 215-kD protein after a 1,000–3,000-fold enrichment of activity. The 215-kD protein, termed *Xenopus* microtubule assembly protein (XMAP), binds to microtubules with a stoichiometry of 0.06 mol/mol tubulin dimer. XMAP is immunologically distinct from the *Xenopus* homologues to mammalian brain microtubule-associated proteins; however, protein species immunologically related to XMAP with different molecular masses are found in *Xenopus* neuronal tissues and testis. XMAP is unusual in that it specifically promotes microtubule assembly at the plus-end. At a molar ratio of 0.01 mol XMAP/mol tubulin the assembly rate of the microtubule plus-end is accelerated 8-fold while the assembly rate of the minus-end is increased only 1.8-fold. Under these conditions XMAP promotes a 10-fold increase in the on-rate constant (from 1.4 $s^{-1} \cdot \mu M^{-1}$ for microtubules assembled from pure tubulin to 15 $s^{-1} \cdot \mu M^{-1}$), and a 10-fold decrease in off-rate constant (from 340 to 34 s^{-1}). Given its stoichiometry in vivo, XMAP must be the major microtubule assembly factor in the *Xenopus* egg. XMAP is phosphorylated during M-phase of both meiotic and mitotic cycles, suggesting that its activity may be regulated during the cell cycle.

One of the most dramatic changes in microtubule assembly and organization in nonneuronal cells occurs during the cell cycle. At the onset of mitosis (or meiosis) the radial array of interphase microtubules is rapidly disassembled, to be replaced by a bipolar spindle that is responsible for chromosome segregation (Brinkley et al., 1976). Although this phenomenon is well studied at the level of morphology, little is known about the regulation of microtubule assembly during the cell cycle. It has been suggested that microtubule-associated proteins (MAPs)[1] serve to regulate microtubule assembly in vivo (for review, see Olmsted, 1986). Immunofluorescence studies have suggested that some MAPs originally identified in brain are present in both interphase and spindle microtubules in cultured nonneuronal cells (Bloom et al., 1984; Connolly et al., 1977, 1978; however, see Izant and McIntosh, 1980). A number of additional MAPs have been identified in nonneuronal cells using criteria such as coassembly with microtubules in vitro (Bulinski and Borisy, 1979), binding to taxol-stabilized microtubules (Vallee, 1982; Vallee and Bloom, 1983), or differential extraction (Duerr et al., 1981). However, little is known regarding the function of these proteins in the regulation of the dramatic transitions in microtubule assembly and organization that occur during the cell cycle.

We have recently studied the regulation of microtubule assembly and organization during the cell cycles of oogenesis and early cleavage in *Xenopus* using cytoplasmic extracts prepared from oocytes and eggs (see preceding article). We reported evidence for two factors that regulate assembly: a plus-end–specific inhibitor of microtubule assembly found only in oocytes, and a plus-end–specific promoter of microtubule assembly in the egg. In this article we present the isolation and preliminary characterization of the plus-end–specific, assembly-promoting factor from eggs. This activity was purified 1,000–3,000-fold, based on its ability to promote nucleated microtubule assembly in vitro, to yield a 215-kD polypeptide that binds to microtubules. We report here on the purification and novel specificity of this factor for the microtubule plus-end.

Materials and Methods

Purification of Microtubule Assembly-promoting Activity from Activated Xenopus Eggs

Xenopus laevis females (20–40) were induced to lay eggs by injection of chorionic gonadotropin (Newport and Kirschner, 1982). Eggs (500–800 ml) were collected by allowing the females to deposit them into 0.1 M NaCl overnight. Eggs were dejellied and activated en masse as previously described (see preceding article). 15 min after activation eggs were rinsed

Address reprint requests to Dr. Kirschner. Dr. Gard's present address is Department of Biology, University of Utah, Salt Lake City, UT 84103.

1. *Abbreviations used in this paper*: BRB, reassembly buffer; MAP, microtubule-associated protein; MPF, maturation-promoting factor; MQ, Mono Q (buffer); MTP, microtubule protein; PC, phosphocellulose column; XMAP, *Xenopus* microtubule assembly protein.

three to five times with cold reassembly buffer (BRB, 80 mM KPipes, 1 mM $MgCl_2$, 1 mM EGTA) containing 1 mM dithiothreitol (DTT), 5 mM NaF, and 1× protease inhibitors (0.1 mM phenylmethylsulfonyl fluoride [PMSF] and benzamidine HCl and 1 μg/ml pepstatin A and phenanthroline). Eggs (100–150 ml after dejellying) were lysed by repeated pipetting (five times with a 25-ml pipette) in 0.2 vol or less excess buffer and were centrifuged at 235,000 *g* for 90 min at 4°C in an SW 50.1 rotor (Beckman Instruments, Inc., Palo Alto, CA). The soluble cytoplasmic proteins were recovered by puncturing the tube with a needle, and collecting the aqueous layer between the yolk and lipid. 700–1000 mg of cytoplasmic protein was typically obtained at 10–15 mg/ml protein.

The protein in the extract was batch adsorbed to phosphocellulose (Whatman, Maidstone, UK) equilibrated in BRB (~30 mg of protein/ml of phosphocellulose) for 3–12 h at 4°C. Phosphocellulose was poured into a column and rinsed with BRB, and bound protein was eluted stepwise with washes of 0.2, 0.3, and 0.5 M NaCl in BRB containing 1 mM DTT and 1× protease inhibitors (Table I). Approximately 16% of the total protein was bound to phosphocellulose, and typically 70–90% of the protein was recovered in the unbound and eluted fractions. Microtubule assembly-promoting activity eluted in the 200–300 mM wash of the phosphocellulose column (PC200–300), which contained 3% of the total recovered protein. The specific activity of the eluted activity was 40–50-fold enriched over the original extract. The total activity recovered in the phosphocellulose elutions was consistently greater than the total activity present in the original extracts, suggesting that the high levels of extract protein assayed actually interfere with assembly. For this reason the activity yield in later purification steps is compared to the total activity in the PC200–300 fraction. Note that this observation may also affect the reported purification factors and yield by as much as twofold.

Activity from the PC200–300 eluate was precipitated by addition of an equal volume of saturated ammonium sulfate (to 50% saturation) at 4°C. Precipitated protein was collected by centrifugation (10,000 *g* for 15 min at 4°C). The resulting pellet was resuspended in Mono Q buffer (MQ buffer: 50 mM imidizole-Cl, pH 6.6, 1 mM MgCl, 1 mM EGTA, 1 mM DTT) with 40 mM NaCl and 1× protease inhibitors, and dialyzed 3 h against the same buffer. After dialysis the protein solution was clarified by centrifugation at 50,000 rpm in a 50Ti rotor for 45 min at 4°C. A substantial loss (50%) of activity and protein occurred during ammonium sulfate precipitation, dialysis, and centrifugation with little increase in specific activity (Table I), apparently owing to nonspecific precipitation. Similar losses were encountered if the PC200–300 was concentrated by ultrafiltration, or was dialyzed directly into MQ buffer or other cationic buffers required for fast protein liquid chromatography (FPLC)-anion exchange chromatography (not shown).

The clarified protein was then applied to a Mono-Q HR 5/5 FPLC anion exchange column (Pharmacia Fine Chemicals, Piscataway, NJ) equilibrated in MQ buffer plus 40 mM NaCl at 0.3 ml/min at 5°C. Bound protein was eluted with a linear gradient of 0–0.6 M NaCl in MQ buffer at 0.5 ml/min. Fractions of 0.5 ml were collected into 0.1 ml of BRB plus 5× protease inhibitors. Aliquots were dialyzed for activity assay (note that imidazole severely inhibits microtubule assembly), and samples were prepared for SDS-PAGE. A single peak of microtubule assembly-promoting activity was obtained eluting at 0.13 M NaCl (Fig. 1 *A*), subsequently referred to as Mono-Q *Xenopus* microtubule assembly protein (XMAP).

The active fractions from the Mono-Q column were pooled and 0.1 vol of 2 M NaCl was added, bringing the total NaCl to ~0.33 M. Protein was then concentrated to 150–200 μl by ultrafiltration in a Centricon 10 device (Amicon Corp., Danvers, MA), requiring ~1 h. Addition of NaCl increased recovery of activity from the concentration step. The concentrated protein was applied to a Biosil TSK400 HPLC size-exclusion column (7.5 × 300 mm; BioRad Laboratories, Richmond, CA) equilibrated in BRB plus 200 mM NaCl, 1 mM DTT, and 1X protease inhibitors. Elution was at 0.5 ml/min and 0.25-ml fractions were collected into 50 μl of BRB plus 5× protease inhibitors. Fractions were dialyzed to BRB plus DTT and protease inhibitors, and assayed for assembly-promoting activity. Aliquots were prepared for SDS-PAGE. A single peak of activity was obtained (Fig. 1 *B*), eluting with an apparent molecular mass of 670–1,000 kD. Active fractions were pooled, and used for assembly experiments. Activity and protein tended to aggregate when frozen, possibly due to the low protein concentrations eluted from the TSK400 column (TSK America Inc., North Bend, WA), usually 50–75 μg/ml. Addition of 100 μg/ml BSA before freezing boosted recovery of activity to 80% after storage at −70°C. Activity was also stable at 4°C overnight (in the presence of protease inhibitors). Protein concentrations were measured according to Bradford (1976), using BSA as a standard. Concentrations of purified XMAP were determined by scanning densitometry of Coomassie-stained SDS-PAGE gels, and compared with known amounts of BSA on the same gel.

Assaying Microtubule Assembly Promotion In Vitro

Promotion of microtubule assembly in vitro was assayed essentially as described previously (see preceding article). Fractions or extracts to be assayed were first dialyzed 2–3 h into BRB plus 1 mM DTT and 1× protease inhibitors. Samples (10–50 μl) were then mixed with phosphocellulose-purified bovine brain tubulin (Mitchison and Kirschner, 1984*b*) and centrosomes from N115 neuroblastoma cells (Mitchison and Kirschner, 1984*a*). Final volume was kept constant by addition of BRB plus 1 mM GTP (to 70 μl). Final tubulin concentrations were 0.7–1.0 mg/ml (7–10 μM). Samples were incubated 5 min at 37°C and microtubules were fixed, sedimented onto coverslips, and visualized by immunofluorescence microscopy (see preceding article). Activity could be estimated visually, using an eyepiece reticle to estimate the diameter of microtubule asters. For quantifying activity more precisely, microtubules were photographed, and 100–200 microtubules were measured to determine the mean microtubule length (± SEM). Specific activities are reported as the difference between the mean length of experimental and control microtubules (assembled with tubulin alone) divided by the amount of protein assayed: $(L_{exp} - L_{ctr})/(\mu g \text{ protein})$. As-

Table I. Purification of XMAP

	Total protein	Sp. act.*	Total activity	Purification	Yield‡
	mg	*per μg protein*			
A. Phosphocellulose chromatography					
Extract	930	0.01	12.1	1	‡
PC fraction/total	630	0	0		
PC0–200	101	0.02	2.1		
PC200–300	31	0.4	12.5	40	1‡
PC300–500	14	0.15	2.1		
MQ load§	12	0.53	6.5	53	0.5‡
B. Summary of purification					
Extract	880	0.006	4.8	1	‡
PC200–300	18	0.3	5.2	50	1‡
MQ XMAP	0.4	2.5	1	420	0.17
TSK XMAP	0.06	18	1	3000	0.17

Parts *A* and *B* are from different experiments. Ranges from several experiments are included in text.
* Specific activity was calculated as $(L_{exp} - L_{ctr})/\mu g$ of protein assayed; see text.
‡ Yields were calculated from the activity recovered in the PC200–300, (see text) and could be overestimated (see Materials and Methods).
§ Protein fraction after ammonium sulfate precipitation, dialysis, and clarification; see text.

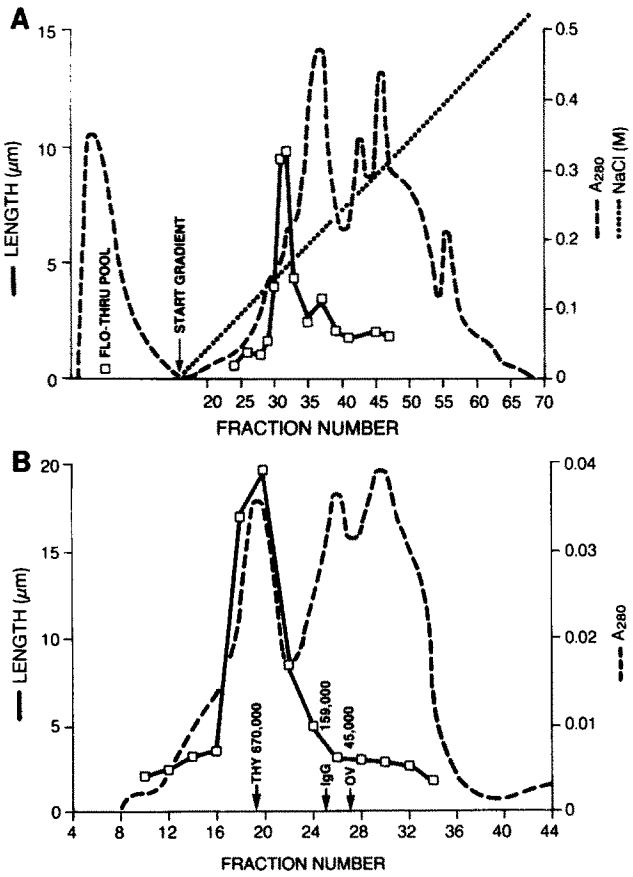

Figure 1. (*A*) Elution profile of assembly-promoting activity from Mono-Q FPLC anion exchange chromatography. Unbound protein was collected in a single pool. Bound protein was eluted with a 0–0.6 M NaCl gradient. The gradient profile (0–0.6 M NaCl, *dotted line*), protein profile (A_{280}, *dashed line*), and assembly-promoting activity (*solid line*) are shown. The length given is the mean length assembled in the fraction assayed minus the mean length of the control microtubules (1.2 μm). A single peak of assembly-promoting activity eluted at 0.13 M NaCl. Assays of the odd fractions between 47 and 60 were visually inspected, and had no assembly-promoting activity. (*B*) Elution profile of assembly-promoting activity from TSK400 HPLC size-exclusion chromatography. The protein profile (A_{280}, *dashed line*) and assembly-promoting activity (*solid line*) are shown. The elution positions of thyroglobulin (670 kD), IgG (159 kD), and ovalbumin (45 kD) are indicated. Assembly-promoting activity eluted as a single peak at or slightly before the elution of the thyroglobulin standard.

sembly rates were determined by dividing mean microtubule lengths by the incubation time. Previous experiments showed that there was no measurable lag in assembly assayed in this manner (Mitchison and Kirschner, 1984*a*, and see Fig. 8). For comparisons of plus- and minus-end assembly, purified *Tetrahymena* axonemes were used in place of centrosomes (Allen and Borisy, 1974; Mitchison and Kirschner, 1984*b*). Bovine brain τ-protein purified by the method of Herzog and Weber (1978), was provided by Dr. David Drubin, Massachusetts Institute of Technology, Cambridge. Other departures from this protocol are described in figure legends or in the text.

Binding of XMAP to Taxol-stabilized Microtubules

Mono-Q XMAP was made 10 μM in taxol, 0.2% in Triton X-100 and was cleared of aggregates by centrifugation (10 min in an airfuge at 95,000 rpm, 4°C). Taxol microtubules were prepared by sequential addition of taxol to 0.1, 1.0, and 10 μM at 5-min intervals (at 37°C) to tubulin at 1 mg/ml (previously cleared of aggregates as above) in BRB. Mono-Q XMAP (amounts indicated in legend) was added to 5 μg of taxol microtubules in a final volume of 0.1 ml BRB (with 10 μM taxol) and was incubated 15 min at 37°C. As controls, mono-Q XMAP and taxol microtubules were incubated separately under identical conditions. Samples were applied to 0.5 ml sucrose cushions (50% wt/vol sucrose in BRB plus 2 μM taxol, 0.1% Triton X-100, and 100 mM NaCl in 5 × 41-mm tubes) and centrifuged 90 min in a SW50.1 rotor at 235,000 *g* (at 20°C). After centrifugation the top of each cushion was removed gently and washed with SDS-PAGE sample buffer. The remaining cushion was then aspirated, and the microtubule pellet was resuspended in SDS-PAGE sample buffer and analyzed by SDS-PAGE. XMAP and tubulin in the pellet were each quantitated by scanning densitometry of Coomassie-stained gels.

Sucrose-Gradient Centrifugation of the 215-kD XMAP Protein

1-ml gradients were prepared from five 0.2-ml steps of 10–40% sucrose in BRB plus 0.2 M NaCl, 1 mM DTT, and 0.02% Triton X-100 and were allowed to linearize for 2 h at 20°C. Mono-Q XMAP (50 μl containing ~15 μg of protein) was applied to the gradient, which was centrifuged 4 h at 55,000 rpm in a TLS55 swinging bucket rotor on a TL-100 centrifuge (Beckman Instruments, Inc.) at 4°C. Ovalbumin (3.6S) and IgG (6S) were included on a parallel gradient as sedimentation standards. Fractions (70 μl) were collected from the top of the gradient and were analyzed by SDS-PAGE. XMAP sedimented to a position corresponding to ~5S.

Determination of XMAP Phosphorylation during Meiotic and Mitotic Cell Cycles

Oocytes were obtained as described (preceding article; Karsenti et al., 1984). Stage VI oocytes (1.1–1.2 mm diam) were incubated for 18 h in 1 mCi/ml $^{32}PO_4$ (New England Nuclear, Boston, MA) in modified Barth saline with Hepes (88 mM NaCl, 1 mM KCl, 1 mM $MgSO_4$, 2 mM $CaCl_4$, 0.1 mM EDTA, 5 mM Hepes, pH 7.8) containing 1 mg/ml BSA. Oocytes were removed from label, and rinsed in modified Barth saline with Hepes. Meiosis was induced by microinjection of 3 U maturation-promoting factor (MPF, Wu and Gerhart, 1980; provided by Dr. Gary Ward of this institution). At intervals after injection samples consisting of six oocytes were rinsed into stop buffer (a buffer which minimizes kinase and phosphatase activity (Gerhart et al., 1984), 26: 50 mM β-glycerophosphate, 50 mM NaF, 10 mM Na pyrophosphate, 10 mM EGTA, and 1× protease inhibitors, pH 7.2), and rapidly lysed in 40 μl of stop buffer. Samples were then frozen in liquid nitrogen until all were collected. A sample of uninjected oocytes was also included. Labeled oocytes were also incubated in cycloheximide (100 μg/ml) for 2 h prior to MPF injection, and assayed for XMAP phosphorylation 3–4 h after MPF injection. After collection of all samples in liquid nitrogen, samples were thawed quickly and yolk was pelleted by centrifugation at 10,000 rpm for 5 min at 4°C. The resulting supernatant was added to an equal volume of SDS-PAGE sample buffer and boiled for 3 min.

Immunoprecipitations were performed as described previously (Gard and Kirschner, 1985), using 3 μl of antiserum to the 215-kD XMAP protein. Because of the changes in overall protein phosphorylation that occur during meiosis and mitosis in the *Xenopus* egg, immunoprecipitations and gel loads were normalized to the total radioactivity in each extract. The incorporation of radiolabel into protein was assayed by TCA precipitation as described (Gard and Kirschner, 1985). Immunoprecipitates were analyzed by SDS-PAGE and autoradiography, and were quantitated by scanning densitometry.

Eggs were fertilized and dejellied, and samples of six eggs each were injected with 50 nl of $^{32}PO_4$ (a total of 40 mCi per egg) as previously described (Karsenti et al., 1987) at 8-min intervals after fertilization. Eggs were allowed to incorporate label for 5 min and were rinsed into stop buffered, lysed, and frozen as above. A sample of unfertilized eggs was also injected with radiolabel and included in the experiment. A sample of fertilized eggs was injected with 50 nl of 200 μg/ml cycloheximide, and then incubated for 2 h in modified Ringers solution plus 200 μg/ml cycloheximide. These eggs, arrested at interphase (Miake-Lye et al., 1983) were injected with label and processed as above.

Preparation of Xenopus Tissue Extracts

Extracts of *Xenopus* tissues were prepared by homogenizing tissues in one volume of BRB plus 1 mM DTT and protease inhibitors. Homogenates were centrifuged for 5 min at 5°C in an airfuge at 30 psi. The resulting supernatants were assayed for protein concentration and prepared for SDS-PAGE.

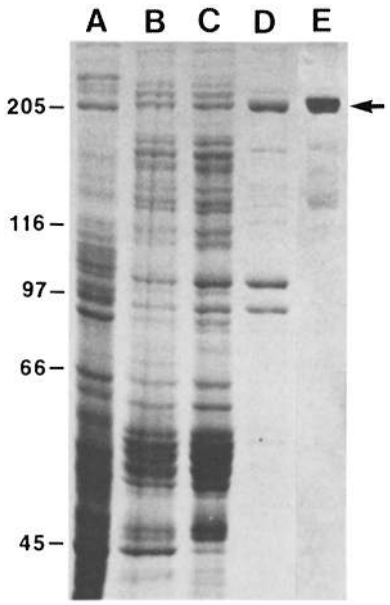

Figure 2. The purified assembly-promoting activity is enriched in a 215-kD polypeptide. Lane *A*, total extract protein (30 μg); lane *B*, PC200–300 (30 μg); lane *C*, protein loaded to the mono-Q column (30 μg); lane *D*, active pool recovered from the mono-Q column (3 μg); lane *E*, final active pool from the TSK400 column (1.5 μg). Lanes *A–D* were Coomassie stained. Lane *E* was silver stained to detect minor proteins. The positions of several molecular mass standards are shown.

Preparation of Antibodies to the 215-kD XMAP Protein

The purified 215-kD XMAP protein was further purified by preparative SDS-PAGE. Stained gel slices containing 75–100 μg of protein were homogenized and emulsified with Freund's complete adjuvant. New Zealand white female rabbits were injected subcutaneously at multiple sites, and were boosted bimonthly with SDS-PAGE–purified antigen in incomplete adjuvant. Sera were tested by immunoblotting against purified XMAP. Sera were ammonium sulfate precipitated to 45% saturation, resuspended, and dialyzed into Tris-buffered saline (10 mM Tris-Cl pH 7.4, 150 mM NaCl) for immunoblotting and immunoprecipitation.

SDS-PAGE and Immunoblotting

SDS-PAGE was on 7 or 8.5% polyacrylamide gels as previously described (Laemmli, 1970; Gard and Kirschner, 1985). Immunoblotting was as described previously using anti-XMAP (1:300 dilution), HMW-3, an antiserum against high molecular mass (HMW) MAPs that primarily reacts with MAP-2 (1:500, Connolly et al., 1978), affinity-purified τ antiserum (1:250, Drubin and Kirschner, 1986), or DMB1 β-tubulin monoclonal antiserum (1:1000, Blose et al., 1984). ^{125}I-labeled *Staphylococcus aureus* protein A (ICN, Irvine, CA) was used in place of secondary antibody (resulting in less background with the frog tissue blots).

Results

In the preceding article we demonstrated that cytoplasmic extracts from activated *Xenopus* eggs support extensive assembly of microtubules in vitro. Freeze-thawing destroyed the ability of the extracts to assemble microtubules; however, these frozen-thawed extracts were capable of promoting the assembly of added purified brain tubulin in vitro (preceding article). Assembly promotion was a linear function of the amount of added egg protein (see Fig. 8 in preceding article), and could be used as a quantitative assay for assembly-promoting activities during subsequent purification. The assembly-promoting activity, termed XMAP (abbreviated from *Xenopus* microtubule assembly protein), was purified from activated eggs through sequential applications of phosphocellulose chromatography, ammonium sulfate precipitation (Table I), FPLC-anion exchange chromatography (Fig. 1 *A*), and HPLC size-exclusion chromatography (Fig. 1 *B*). A summary of the purification and yields is shown in Table I, and SDS-PAGE analysis of the resulting protein fractions is shown in Fig. 2. The major loss of activity and protein occurred after ammonium sulfate precipitation and dialysis into a cationic buffer for FPLC-anion exchange chromatography (see Materials and Methods). Microtubule assembly-promoting activity eluted as a single peak in both the anion exchange and size-exclusion steps (Fig. 1). Purification of assembly-promoting activity correlates with enrichment of a 215,000 M_r polypeptide that represents 90–95% of the protein of active fractions from the size-exclusion column (Fig. 2). The final yield after size-exclusion chromatography was typically 50–100 μg of protein, representing 5–20% of the total activity with a purification factor of 1,000–3,000-fold. Assembly activity was not heat stable, and was inactivated by 5 min of incubation at 100°C (not shown).

To demonstrate directly the binding of the 215-kD polypeptide to microtubules, a partially purified fraction from the mono-Q step, (mono-Q XMAP, of which the 215-kD protein represents ~20%) was incubated with and without taxol-stabilized microtubules assembled from bovine brain tubulin. The resulting microtubules were analyzed by SDS-PAGE after centrifugation through a sucrose cushion to separate bound and unbound proteins (see Materials and Methods) (Fig. 3). No protein from the mono-Q XMAP sedimented through the sucrose cushion in the absence of microtubules (lane *C*). A substantial amount of the 215-kD polypeptide specifically cosedimented with the taxol-stabilized microtubules (lane *D*). Comparison with lane *A* indicates that at least one-third to one-half of the 215-kD protein present in the incubation was recovered in the microtubule pellet. The lack of sedimentation of other proteins from the mono-Q XMAP fraction indicates that the interaction of the 215-kD protein with microtubules is specific, and not due to nonspecific protein aggregation.

Note that the mono-Q XMAP also enhanced the recovery of tubulin in the microtubule pellet (compare lanes *B* and *D*), suggesting that XMAP affects tubulin assembly and stabilization at very low tubulin concentrations, even in the presence of taxol.

In a similar experiment increasing amounts of the mono-Q fraction were incubated with a constant amount of taxol microtubules. Binding of the 215-kD polypeptide to taxol-stabilized microtubules reaches apparent saturation at ~6 mol per 100 mol tubulin dimer (0.06 mol/mol). All subsequent stoichiometries reported are moles of XMAP to moles of tubulin dimer (α and β) assuming molecular masses of 215 kD for XMAP and 100 kD for tubulin dimer.

Size-exclusion chromatography indicates an apparent native molecular mass of 670–1,000 kD for the microtubule assembly-promoting activity (Fig. 1 *B*), which is significantly larger than the 215-kD molecular mass of the XMAP polypeptide determined by denaturing SDS-PAGE (Fig. 2). XMAP was subjected to sucrose gradient sedimentation to determine whether it was an asymmetric or multimeric protein. XMAP sedimented with a mobility intermediate between that of ovalbumin (3.6S) and IgG (6S), providing a

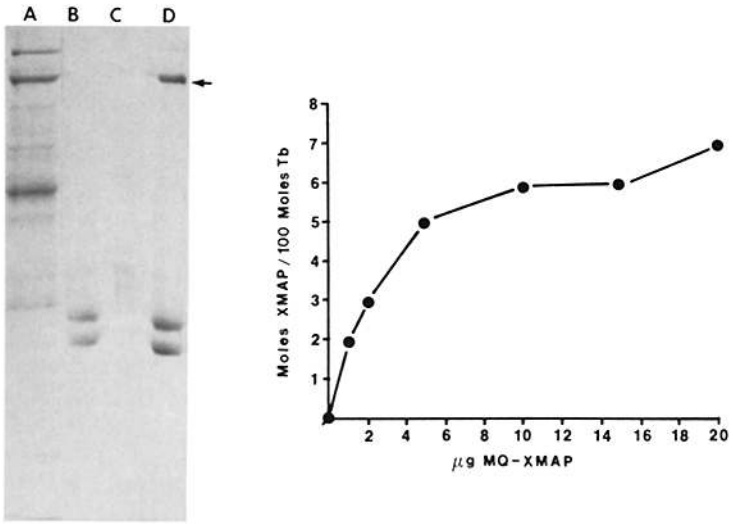

Figure 3. The 215-kD protein binds to taxol-stabilized microtubules. Lane *A*, 5 μg of mono-Q XMAP after removal of aggregates by centrifugation; lane *B*, pellet from 5 μg of taxol-stabilized microtubules; lane *C*, pellet from 15 μg of the mono-Q protein incubated without microtubules; lane *D*, pellet from 15 μg of mono-Q protein incubated with 5 μg of taxol-stabilized microtubules. The 215-kD protein specifically cosediments with microtubules. A similar experiment was used to quantitate the stoichiometry of binding of the 215-kD polypeptide (XMAP) to taxol-stabilized microtubules. The molar ratio of XMAP to tubulin in the microtubule pellet is plotted against the amount of the mono-Q XMAP added to 5 μg of taxol microtubules. XMAP binding saturates at ~6 mol per 100 mol tubulin dimer.

sedimentation coefficient of ~5S for the 215-kD protein. From this value, and the diffusion coefficient ($2.2 \times 10^{-7} \cdot cm^2 \cdot s^{-1}$) determined by size-exclusion chromatography, a native molecular mass of 205 kD was calculated, with an axial ratio of ~40–70:1 ($f/f_0 = 2.7$).

Distribution of XMAP in Xenopus Tissues

A rabbit polyclonal antiserum to the 215-kD XMAP protein was prepared and used to probe immunoblots containing purified XMAP, total egg extract, extracts of several tissues from *Xenopus*, and bovine brain microtubule protein (MTP)

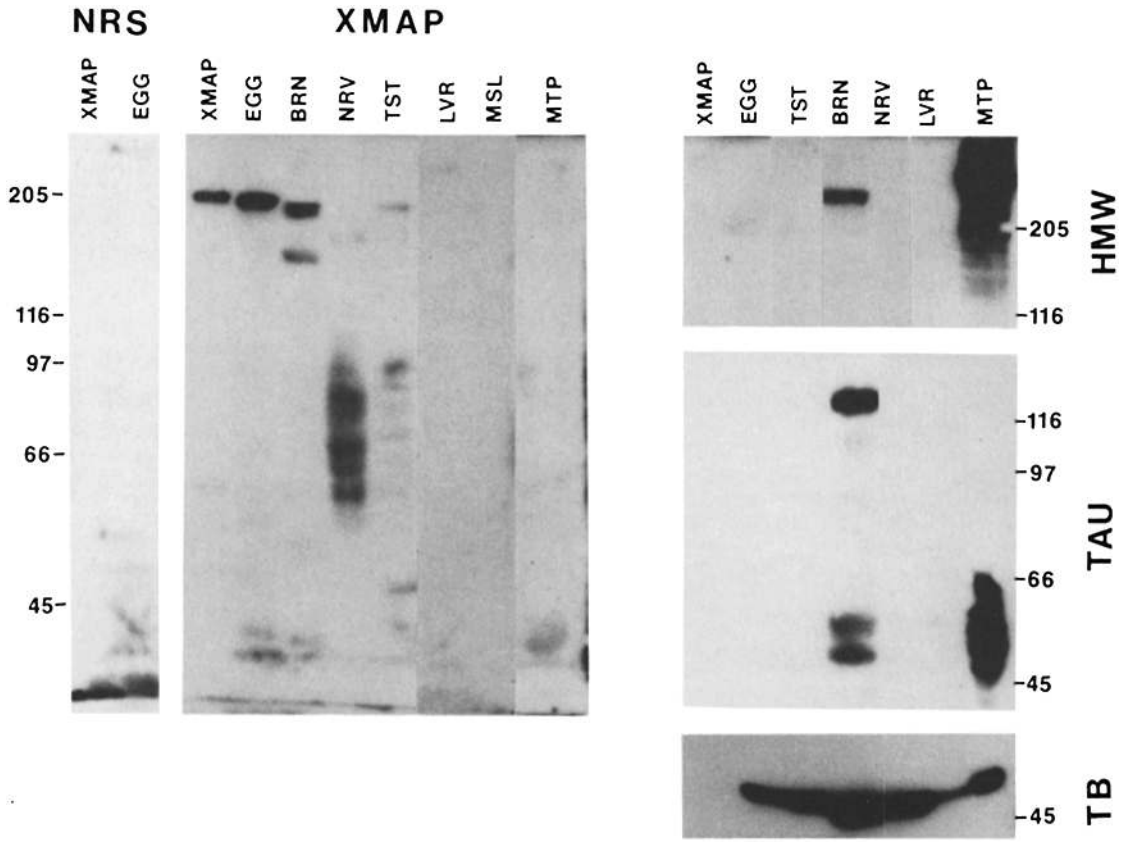

Figure 4. Immunoblot identification of XMAP in *Xenopus* tissues. Purified XMAP (30 ng), *Xenopus* tissue extracts (50 μg each), and bovine brain microtubule protein (*MTP*, 5 μg for HMW, 5 μg for τ, and 1.3 μg for tubulin antisera) were immunoblotted with normal rabbit serum (*NRS*, only XMAP and egg extract shown), or antiserum to XMAP, porcine brain HMW-MAPs (*HMW*), bovine brain τ (*TAU*), or β-tubulin (*TB*). Tissues examined were total egg extract (*EGG*, see Fig. 2 for protein profile of egg extract), brain (*BRN*), spinal cord (not shown), sciatic nerve (*NRV*), testis (*TST*), liver (*LVR*), and skeletal muscle (*MSL*, not shown for *HMW, TAU, TB*). The entire gel is shown for the XMAP antiserum. Only those regions of the gel exhibiting reactive proteins are shown for the HMW, τ, and tubulin sera. These gels have been arranged such that the lanes correspond for all antisera. The positions of the protein molecular mass standard are indicated. A summary of this figure is presented in Table II.

Table II. Distribution of XMAP and Brain MAPs in Xenopus Tissues

Tissue	Antiserum			
	XMAP	HMW*	Tau‡	Tb§
TSK-XMAP	++++(215)	–	–	–
Egg	++++(215)	–	–	+
Testis	+(200, 80–90)	–	–	++
Brain	++(195–200, 155)	+(240–250)	++(130, 60–70)	++++
Spinal cord	+(as brain)	+(as brain)	+(130)	+++
Peripheral nerve	+++(64–105)	–	–	++
Liver	–	–	–	+
Skeletal muscle	–	–	–	+
Microtubule protein	–	++++	++++	++++

Molecular masses are in kilodaltons (values parenthesized). Reaction to each antibody was judged on a qualitative scale from no reaction (–) to strong reaction (++++).
* Primarily recognizes MAP-2 by immunoblotting (see text).
‡ Affinity purified.
§ Monoclonal antibody to β-tubulin.

(Fig. 4). XMAP antiserum reacted strongly with purified XMAP (30 ng). The XMAP antiserum detected a single protein in total egg extract (*EGG*, 50 μg loaded, see Fig. 2, lane *A* for the protein profile of total egg protein) that comigrates with 215-kD XMAP. This 215-kD XMAP protein was the only species detected by immunoblotting of egg proteins solubilized directly in SDS-PAGE sample buffer, indicating that it is not generated by proteolysis of a larger protein during sample preparation (not shown). Preimmune serum did not react with XMAP, egg extract or extracts from other tissues. From the intensities of the antiserum reaction to purified XMAP and XMAP in total egg extract (determined by scanning densitometry), we estimate that XMAP represents 0.15% of the total soluble protein in the egg.

XMAP antiserum did not react with any proteins present in bovine brain MTP (*MTP*, containing HMW-MAPs-1 and -2, τ-proteins, and tubulin). Conversely, neither antiserum to porcine brain HMW MAPs (Connolly et al., 1978) or affinity-purified antiserum to bovine brain τ-protein (Drubin et al., 1986) reacted with purified XMAP, or to any protein species in *Xenopus* eggs (Fig. 4, *right*).

XMAP antiserum did react with protein species with distinct molecular masses in frog brain (*BRN*, a doublet of 195–200 kD, and a 155-kD protein), spinal cord (the same species as brain, not shown), peripheral nerve (*NRV*, a strong reaction to multiple species of 64–105 kD), and testis (*TST*, a weak reaction to proteins of 200 and 80–90 kD). No cross-reactive species were present in liver (*LVR*) or muscle (*MSL*). We immunoblotted the same spectrum of *Xenopus* tissues with antisera to porcine HMW MAPs (Connolly et al., 1978), bovine τ-protein (Drubin et al., 1986), and β-tubulin (Blose et al., 1984). The HMW antiserum reacted with a doublet of 240–250 kD in *Xenopus* brain and spinal cord which were distinct from the 195–200-kD proteins in brain

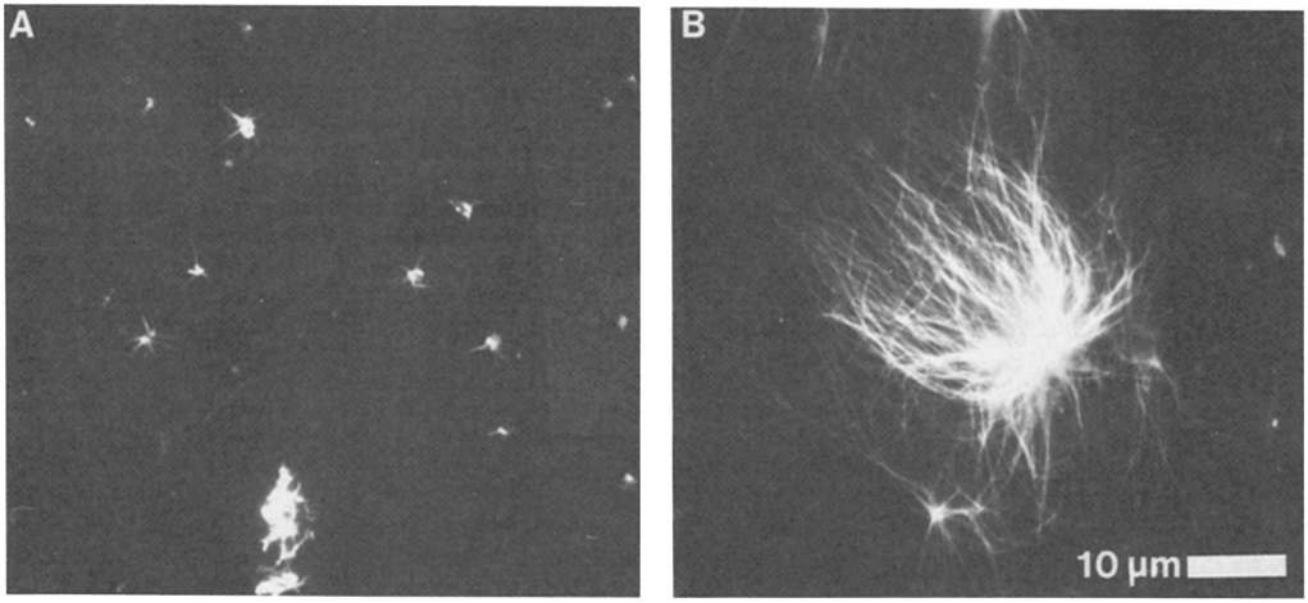

Figure 5. XMAP dramatically promotes assembly of tubulin from centrosomes. Centrosomes were incubated in 0.93 mg/ml purified brain tubulin for 5 min at 37°C in the (*A*) absence or (*B*) presence of purified XMAP at a final concentration of 0.023 mg/ml (resulting in a molar ratio of 0.012 mol XMAP/mol tubulin). Microtubules were fixed and visualized by immunofluorescence with antitubulin. Bar, 10 μm.

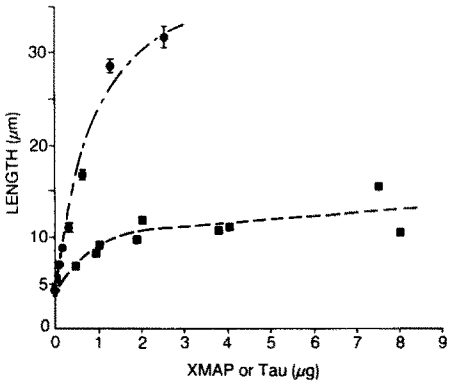

Figure 6. Comparison of the assembly-promoting activity of purified XMAP and bovine τ-proteins. Tubulin assembly from centrosomes (0.71 mg/ml for 10 min at 37°C) was assayed in the presence of increasing amounts of XMAP (●) or tau proteins (■). Microtubules were fixed, visualized by immunofluorescence with antitubulin, photographed, and measured. The mean lengths are shown. Error bars have been omitted, however, in all cases the SEM was <5% of the mean.

recognized by the XMAP antiserum. The HMW antiserum recognized primarily MAP-2 and its proteolysis products in MTP (highly overexposed in the blot shown), and reacted only weakly with MAP-1. τ-Antiserum reacted with species of 130 and 60–70 kD in *Xenopus* brain, and 130 kD in spinal cord. Neither MAP serum reacted with peripheral nerve, testis, liver, or muscle. Neither HMW or τ-antisera reacted with any of the various proteins recognized by the XMAP antiserum in any tissue. Tubulin antiserum reacted with all tissues (but did not react with purified XMAP). These results are summarized in Table II. By normalizing the reaction of XMAP antiserum in various tissues to the amount of tubulin, it is apparent that, except for the strong reaction in peripheral nerve, the ratio of XMAP antigen to tubulin is significantly higher in eggs than in any other tissue (3–10-fold greater than brain, 60–100-fold greater than testis, and more than 100-fold greater than liver or muscle).

XMAP Is a Potent Promoter of Microtubule Elongation

All subsequent experiments were performed with XMAP purified to 90–95% homogeneity. Addition of XMAP to tubulin and centrosomes (0.023 mg/ml XMAP and 0.93 mg/ml tubulin, a molar ratio of 0.012) resulted in a significant increase in the length of microtubules assembled in a 5-min incubation at 37°C (from 2.3 ± 0.1 to 16.7 ± 0.5 μm, Fig. 5). Because centrosomes are provided as a nucleation center and there is no apparent lag in assembly (see below), this must be due to an increase in the microtubule elongation rate.

A comparison of the effect of added XMAP on assembly with that of τ-protein (a MAP from bovine brain; Cleveland et al., 1977) is shown in Fig. 6. Addition of τ-protein produced a maximal increase of twofold in microtubule assembly rate, as evident by the length of microtubules assembled. This stimulation was achieved when 2 μg of purified τ was added, corresponding to a molar ratio of 0.067 mol tau/mol tubulin. In comparison, 1.5 μg of added XMAP (a molar ratio of 0.014 mol/mol tubulin) promoted nearly a sixfold increase in microtubule length. The apparent saturation of the

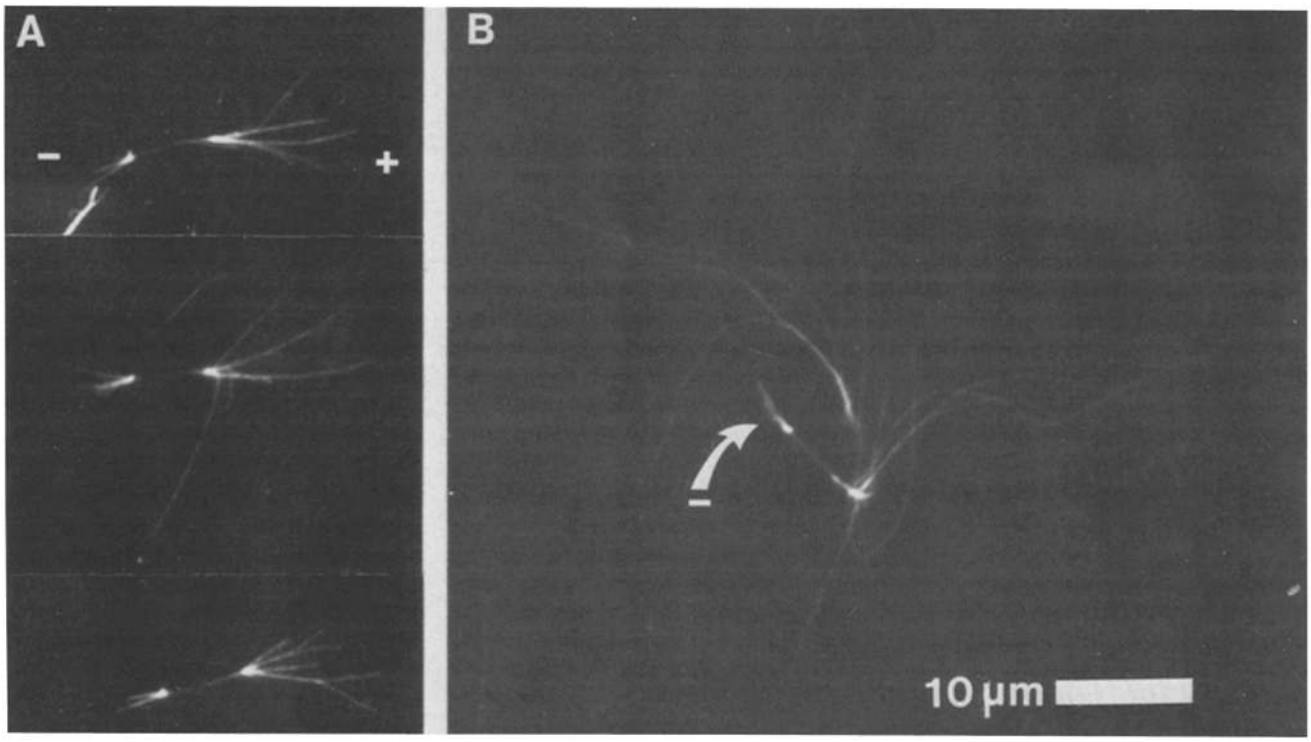

Figure 7. XMAP preferentially promotes plus-end assembly of microtubules. Tetrahymena axonemes were used to nucleate microtubule assembly in the absence (*A*, 0.93 mg/ml tubulin for 10 min at 37°C) or presence of XMAP (*B*, 0.023 mg/ml XMAP, 0.93 mg/ml tubulin for 3 min at 37°C). Bar, 10 μm.

effect of XMAP on tubulin assembly at this low stoichiometry is most likely an artifact owing to shearing of the excessively long microtubules obtained with higher molar ratios of XMAP. Binding to taxol microtubules (above) suggests that saturation would occur at the fourfold higher ratio of 0.06 mol XMAP/mol tubulin.

XMAP Specifically Affects Assembly at the Microtubule Plus-End

When *Tetrahymena* axonemes were used to nucleate microtubule assembly in the presence of purified XMAP, it was apparent that XMAP had its predominant effect at the plus-end. After 3 min of assembly with tubulin and XMAP (at a molar ratio of 0.012 mol/mol tubulin) plus-end microtubules reached a mean length of 16.0 ± 0.8 μm, whereas minus-end microtubules reached a mean length of only 1.2 ± 0.1 μm, giving a ratio of plus- to minus-end length of 13.3 (Fig. 7). In a 10-min assembly with pure tubulin, plus-end microtubules reached a mean length of 5.1 ± 0.2 μm, whereas minus-end assembly was only 2.2 ± 0.1 μm, giving a ratio of plus- to minus-end lengths of 2.3.

To further study the end specificity of XMAP we examined the ratio of plus- to minus-end assembly rates (from axonemes) as a function of increasing amounts of either XMAP or bovine brain τ-protein with a constant concentration of tubulin (Fig. 8). The ratio of plus- to minus-end microtubule length remained constant with increasing amounts of added τ-protein (*circles*). The highest amounts of tau assayed were threefold greater than those found to maximally affect assembly (Fig. 6). In contrast, increasing amounts of XMAP promoted a large increase in the ratio of plus- to minus-end lengths (*squares*). The plus-end–specific nature of XMAP has been observed with several different preparations of tubulin and XMAP, whereas τ-protein never showed end-specific effects.

In a subsequent experiment microtubule length was assayed at several intervals during assembly from axonemes in the presence or absence of XMAP (Fig. 8 *B*). Control microtubules exhibited assembly rates of 0.4 and 0.15 $\mu m \cdot min^{-1}$ for the plus- and minus-ends, respectively. The corresponding assembly rates in the presence of XMAP (0.012 mol/mol tubulin) were 3.2 and 0.26 $\mu m \cdot min^{-1}$. The dramatic increase in the plus-end assembly rate results in a 12-fold difference in the rates of assembly of the plus- and minus-ends in the presence of XMAP, compared with the 2.7-fold difference in control microtubules. Note that no lag phase was observed in assembly nucleated by axonemes (or by centrosomes, not shown).

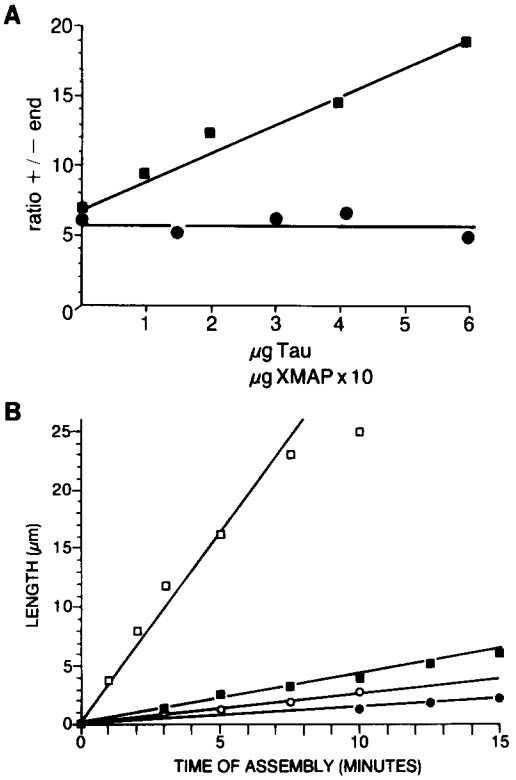

Figure 8. XMAP preferentially promotes assembly at the microtubule plus-end. (*A*) Microtubules were assembled from axonemes and tubulin (0.7 mg/ml for 10 min at 37°C) in the presence of the indicated amounts of purified bovine brain τ-protein (●) or XMAP (■). Note the 10-fold difference in scale for the two assembly factors. Microtubules were photographed and measured, and the ratio of the lengths of microtubule ends is shown for each point (plus/minus). Control microtubule lengths were 6 ± 0.2 and 1 ± 0.1 μm for the plus- and minus-ends, respectively. At 6 μg of added τ (0.2 mol/mol tubulin) the corresponding lengths were 11.4 ± 0.2 and 2.3 ± 0.1 μm. At 0.6 μg of XMAP (0.006 mol/mol) the lengths were 19.2 ± 0.6 and 1.0 ± 0.1 μm. Note that in the absence of added τ-protein or XMAP the ratio of plus- to minus-end microtubule lengths was higher in the experiments shown in *A* than that in experiments described in Fig. 7 (q.v.) or described below. This difference was due to one particular batch of purified tubulin used which exhibited a greater disparity in the assembly rates at the plus- and minus-ends. This did not affect the results of the experiments with added assembly factors. (*B*) Microtubules were assembled from axonemes (0.93 mg/ml tubulin) in the absence (*solid symbols*) or presence of XMAP (0.023 mg/ml, corresponding to 0.012 mol/mol tubulin, *open symbols*). Assembly was for the indicated times, at which point aliquots were withdrawn and fixed for immunofluorescence. The mean lengths (n = 100–200) of plus- (*squares*) and minus-ends (*circles*) are shown. SEM are omitted, but were <5% of the mean.

XMAP Affects Both On- and Off-Rate Constants of the Microtubule Plus-End

The on-rate for plus-end microtubule assembly (from centrosomes) was determined by measuring the dependence of assembly rate on tubulin concentration with or without a constant molar ratio (0.012 mol/mol tubulin) of purified XMAP (Fig. 9 *A*). We chose such a low stoichiometry of XMAP to tubulin so that the growth rates could be accurately measured. The on-rate constant for assembly at the plus-end of control microtubules was 0.05 $\mu m \cdot min^{-1} \cdot \mu M^{-1}$, or 1.4 $s^{-1} \cdot \mu M^{-1}$. This value is approximately half that measured by Mitchison and Kirschner (1984*b*), possibly owing to variability in tubulin preparations. Even at the low stoichiometry used (0.012 mol/mol tubulin) XMAP promoted a 10-fold increase in the tubulin on-rate at the plus-end to 0.5 $\mu m \cdot min^{-1} \cdot \mu M^{-1}$ (15 $s^{-1} \cdot \mu M^{-1}$).

The off-rate constant for the microtubule plus-end was determined by measuring the rate of microtubule disassembly after dilution (Fig. 9 *B*). Assembly from centrosomes assures that only plus-end disassembly was observed. After a transient rapid disassembly of ~2 μm (<20% of their length,

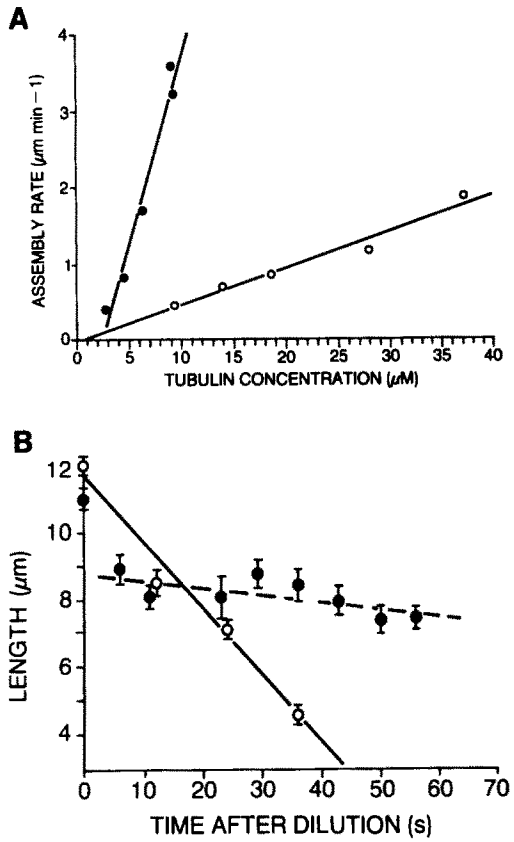

Figure 9. XMAP affects both the on- and off-rates at the microtubule plus-end. (*A*) The rates of microtubule assembly from centrosomes were determined for increasing concentrations of tubulin (1 mg/ml equals 10 μM) in the absence (○) or presence (●) of a constant stoichiometry of XMAP (0.012 mol/mol tubulin). A least squares curve fitting program was used to determine the slope of the rate dependence on tubulin concentration, which represents the rate constant for tubulin addition (see text). (*B*) Centrosomal microtubules were assembled (0.6 mg/ml tubulin) in the absence (○) or presence of XMAP (0.013 mg/ml, corresponding to 0.01 mol/mol tubulin, ●). An aliquot was removed for fixation and the remaining samples were rapidly diluted into 25 vol of BRB at 37°C, without or with 0.013 mg/ml XMAP, respectively. Aliquots were withdrawn and fixed for immunofluorescence at the indicated times.

possibly because of shearing during dilution) microtubules disassembled at a rate of 0.02 $\mu m \cdot s^{-1}$ (34 s^{-1}). Microtubules assembled from pure tubulin disassembled at a rate of 0.2 $\mu m \cdot s^{-1}$ (340 s^{-1}).

Cell Cycle Regulation of XMAP Phosphorylation

We examined XMAP phosphorylation during both the meiotic and mitotic cell cycles in oocytes and eggs. As reported by Maller et al. (1977), overall levels of protein phosphorylation increase during meiosis, indicated by the overall intensity of label incorporation in the total oocyte extracts after MPF injection (Fig. 10 *A*). [^{32}P]XMAP is undetectable by immunoprecipitation in immature oocytes, although XMAP itself is present in oocytes at levels comparable to those of eggs (determined by immunoblotting, not shown). By 27 min after MPF injection [^{32}P]XMAP is just detectable, and levels of labeled XMAP continue to rise until 75 min after injection. This first peak in XMAP phosphorylation corresponds in time to first meiotic metaphase (Gerhart et al., 1984). Thereafter [^{32}P]XMAP falls briefly (to a low at 90 min), corresponding to interphase between meiosis I and II, and then rises to a maximum level at 180–240 min as the oocytes arrest at second meiotic metaphase. These results were confirmed by quantitation of a similar experiment (Fig. 10 *B*). Because oocytes were labeled for a period longer than required to reach steady state (Maller et al., 1977) and incorporation of $^{32}PO_4$ into ATP does not change substantially during maturation, these fluctuations in $^{32}PO_4$ incorporation into XMAP represent actual regulation of XMAP phosphorylation. Oocytes incubated in cycloheximide prior to MPF injection (and maintained in cycloheximide) exhibit minimal incorporation of $^{32}PO_4$ into XMAP. Cycloheximide has been shown to block cells in meiotic interphase (Miake-Lye et al., 1983), with no effect on overall levels of protein phosphorylation (Karsenti et al., 1987).

To assay XMAP phosphorylation and phosphate turnover during the mitotic cycles of cleaving eggs, fertilized eggs were labeled as described in Materials and Methods. Incorporation of $^{32}PO_4$ into XMAP was maximal in unfertilized eggs arrested at meiotic metaphase II, as expected from the results of the previous experiment (Fig. 10 *C*). $^{32}PO_4$ XMAP falls to 30% of the maximal value by 50 min (0.52, the time required for dejellying and injecting the eggs). Peaks in incorporation of $^{32}PO_4$ into XMAP are apparent at 0.8 and 1.1, corresponding to mitotic metaphase of the first two cell cycles (Gerhart et al., 1984). The slight increase observed in the last time point taken (at 1.45) probably represents the initiation of the third mitotic metaphase.

If eggs are microinjected with cycloheximide immediately after fertilization they arrest in S-phase between the first and second mitoses (Miake-Lye et al., 1983). When labeled by microinjection of phosphate at the indicated time such arrested eggs exhibit minimal levels of [$^{32}PO_4$]XMAP. Immunoprecipitation of [^{32}P]XMAP normalized to the TCA-precipitable label in the extracts also exhibited cyclic increases of [^{32}P]XMAP corresponding to mitotic metaphase, indicating that the cell cycle-dependent variations of XMAP phosphorylation were greater than the overall changes in protein phosphorylation (not shown).

Discussion

In the preceding article we showed that *Xenopus* oocytes and eggs contain two modulators of microtubule assembly: an inhibitor of microtubule assembly in oocytes and a promoter of microtubule elongation in activated eggs. In this article we show that purified assembly factor from activated eggs has novel properties that explain the microtubule assembly properties found in cytoplasmic extracts. We followed the purification of microtubule assembly-promoting activity by using a functional assay so that we could assess the contribution of any purified factors to the overall assembly-promoting activity in the egg. This assay, measuring the promotion of tubulin assembly from isolated centrosomes, is specific for microtubule elongation and does not assay microtubule nucleation.

Assembly-promoting activity was purified 1,000–3,000-fold through successive chromatographic procedures, with a recovery of activity of 5–20%. The resulting active fraction was enriched in a polypeptide of 215 kD (representing

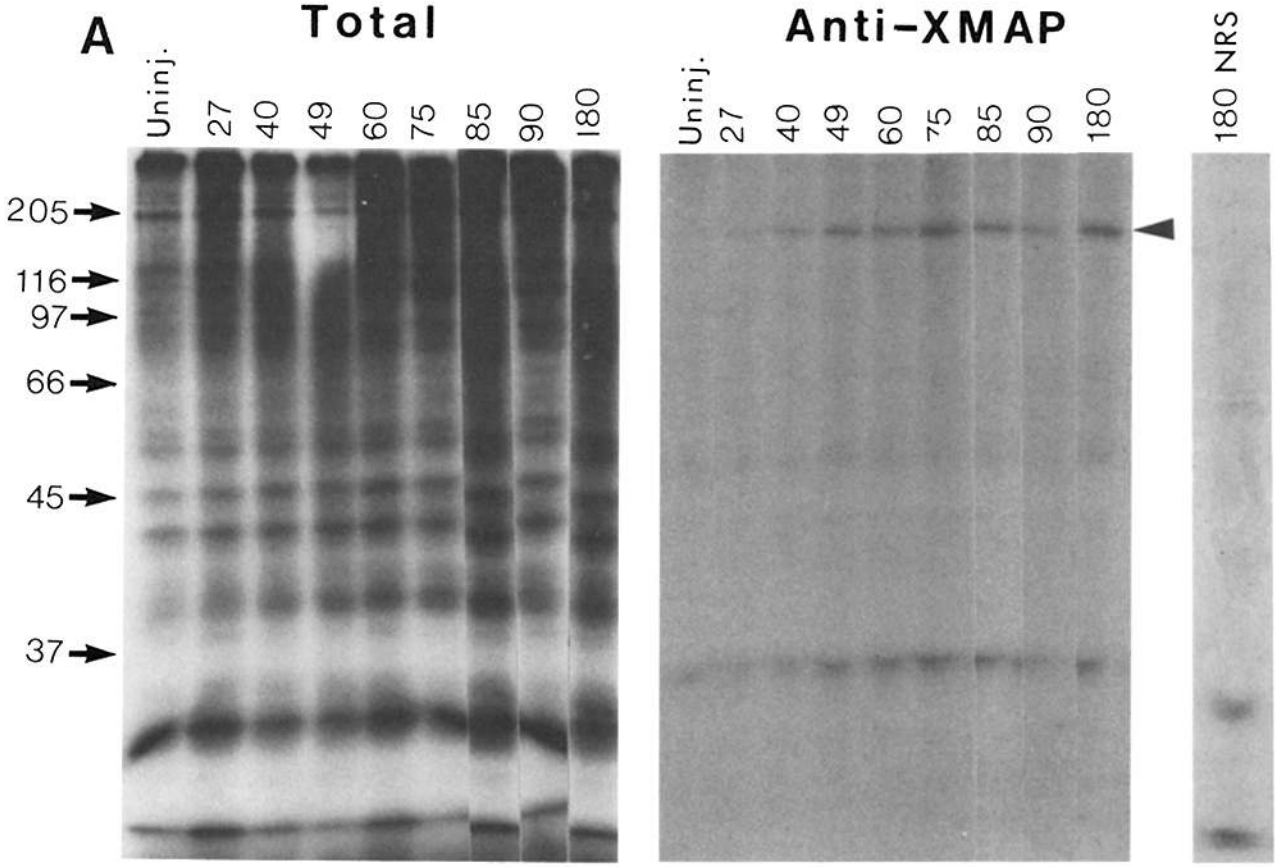

Figure 10. Phosphorylation of XMAP is regulated during the meiotic and mitotic cell cycles. (*A*) Oocytes were labeled with ^{32}P and injected with MPF as described in Materials and Methods and Results. The total protein profile (*Total*, 3.9×10^5 cpm per lane on an 8.5% gel, exposed 2 d without screen) and immunoprecipitated XMAP (*Anti-XMAP*, 3.9×10^6 cpm immunoprecipitated, a 7% gel, exposed 10 d with screen) are shown. Lanes are labeled by the time after MPF injection (Uninj, oocytes not injected with MPF). The position of protein standards are shown. Immunoprecipitated XMAP migrates with a molecular mass of 215 kD, just above the 205-kD standard. A labeled protein of ~40 kD was apparent in all lanes, and is presumed to be nonspecifically adsorbed during the immunoprecipitation since it was also observed with normal rabbit serum (*180 NRS*, normal rabbit serum precipitation of the 180-min sample). *Opposite page*: (*B*) The autoradiograph from a similar experiment was quantitated by scanning densitometry. Results are plotted as per cent maximal levels of [^{32}P]XMAP vs. time after MPF injection. Peaks in [^{32}P]XMAP correspond in time to meiotic metaphase I and II. Cycloheximide-arrested oocytes exhibit low [^{32}P]XMAP (○). The time of 50% nuclear envelope breakdown (germinal vesicle breakdown, *GVBD*) is shown. (*C*) Incorporation of $^{32}PO_4$ into XMAP is regulated during cleavage. Eggs were labeled for 5 min by microinjection of $^{32}PO_4$ and [^{32}P]XMAP was assayed as described in the text. [^{32}P]XMAP is reported as the percentage of the maximal value observed in unfertilized eggs (*UNF*) vs. time after fertilization at which the eggs were injected with label (times are normalized to first cleavage such that 1.0 equals 96 min). Levels of [^{32}P]XMAP peaked at 0.7 and 1.1 of the cleavage cycle, corresponding to mitotic metaphase (*M*). The declining height of successive peaks of [^{32}P]XMAP may be due to the successive loss of synchrony in the cell cycles of the eggs sampled during the course of the experiment. Similar results were obtained in two independent experiments. Eggs arrested in interphase by incubation in cycloheximide prior to injection of $^{32}PO_4$ at the indicated time exhibit minimal incorporation into XMAP (★).

90–95% of the protein present in the fraction), which we have designated XMAP.

There does not appear to be any cross-reaction between XMAP and antiserum to HMW-MAPS or τ-proteins, or conversely, between brain microtubule protein (HMW-MAPs-1 and -2, τ-proteins, or tubulin) and antiserum to XMAP. Among the *Xenopus* tissues examined (oocyte, egg, brain, spinal cord, peripheral nerve, testis, liver, and skeletal muscle) the 215-kD XMAP protein is restricted to eggs and oocytes. Preliminary evidence indicates that the 215-kD XMAP protein accumulates during oogenesis and is lost during early embryogenesis (around late neurula stage, unpublished observations), suggesting that it represents an embryonic microtubule assembly protein.

The XMAP antiserum does detect cross-reactive proteins of distinct molecular mass in several *Xenopus* tissues. None of these forms are recognized by antisera to porcine brain MAP-1 or bovine τ-proteins. We have yet to determine the relationship between the distinct tissue forms of XMAP in *Xenopus*. In addition, the relationship between XMAP and other identified microtubule-associated proteins, such as MAPs-1 and 3–5 from mammalian brain (Olmsted, 1986), the proteins identified by microtubule binding in *Xenopus* oocytes (Jessus et al., 1985) and sea urchin eggs (Vallee and Bloom, 1983), and similarly sized MAPs from cultured cells such as MAP-4 (Bulinski and Borisy, 1979; Olmsted, 1986) remains to be firmly established.

The 215-kD XMAP polypeptide binds to and cosediments

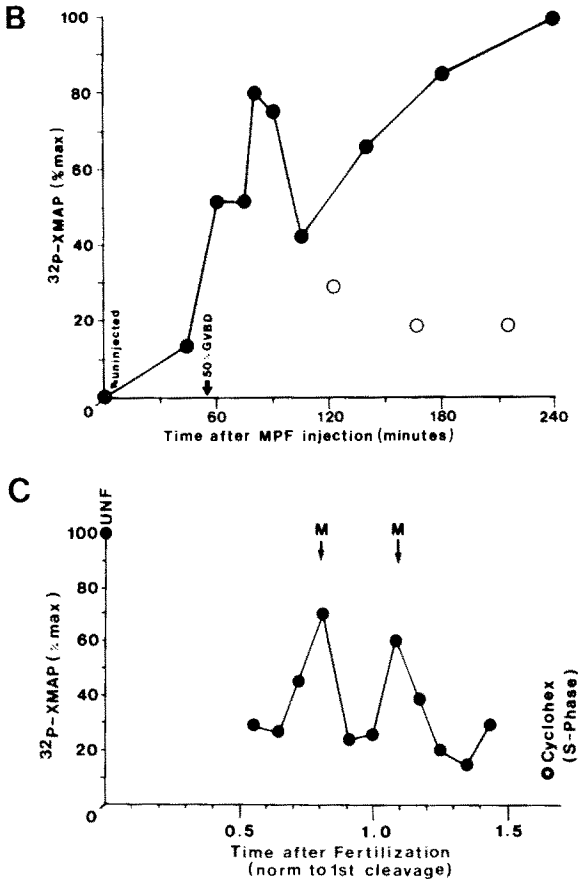

Figure 10

with taxol-stabilized microtubules with apparent saturation occurring at 0.06 mol per mol tubulin dimer. This stoichiometry is less than that observed for the HMW MAPs and τ-proteins in brain (typically ~0.16 mol/mol tubulin; Cleveland et al., 1977; Kim et al., 1979). The observed binding ratio suggests that XMAP binds along the entire microtubule length, either longitudinally or circumferentially. This conclusion is also supported by the observation of microtubule cross-linking and bundling by XMAP by using immunofluorescence and electron microscopy (unpublished observations).

XMAP behaves as an asymmetric monomer of the 215-kD protein in solution. From size-exclusion chromatography and sucrose-gradient sedimentation, we calculate that XMAP has an axial ratio of 40–70:1 (f/f_0 = 2.7). Using a protein density of 1.15 g·cm^{-3} and assuming from the axial ratio that XMAP is roughly cylindrical, we calculate an approximate length for XMAP of 100 nm. A molecule of this length could interact with as many as 13 tubulin subunits in either a longitudinal or circumferential binding to the microtubule. This estimate is in close agreement with the binding stoichiometry observed (0.06 mol XMAP/mol tubulin).

Based on the average recovery of activity (~5–20%) and protein (50–100 μg from ~1,000 mg of total soluble egg protein) from several XMAP preparations, we estimate that the 215-kD XMAP protein represents 0.03–0.2% of the total soluble protein in the egg. Immunoblotting with antibody specific for the 215-kD XMAP protein suggests that it represents 0.15% of the total soluble protein. Using the latter figure and previous estimates of the tubulin content in the egg (2.8% of the soluble protein; see preceding article), we calculate a molar ratio of XMAP to tubulin 0.025 mol/mol in the intact egg. This estimate is within a factor of three of the maximum binding stoichiometry observed in vitro, and suggests that XMAP binds with a high stoichiometry to microtubules in the egg.

XMAP is a potent promoter of microtubule assembly in vitro. Assuming that the effect of XMAP on the assembly rate is a linear function of XMAP concentration, and with knowledge of its concentration in vivo, we project an on-rate constant for tubulin assembly in the egg (at 37°C) of 33 $s^{-1}\cdot\mu M^{-1}$. If XMAP were present at saturating levels in the egg the on-rate constant (at 37°C) would be 76 $s^{-1}\cdot\mu M^{-1}$. Even considering the differences in temperature used, the assembly rate constants yielded by purified XMAP and tubulin compare favorably with the 57 $s^{-1}\cdot\mu M^{-1}$ estimated for egg cytoplasm at 22°C (preceding article). This correspondence supports our conclusion that XMAP represents the major factor promoting microtubule assembly in *Xenopus* eggs. At the tubulin concentrations in the egg (20–25 μM; see preceding article) these on-rate constants would correspond to a rate of microtubule assembly of 23–67 $\mu m\cdot min^{-1}$. Such a rapid rate of assembly is sufficient to account for the observed rate of assembly of the sperm aster after fertilization (30–50 $\mu m\cdot min^{-1}$; Manes and Barbieri, 1977; Stewart-Savage and Grey, 1982).

A striking feature of XMAP is the specific promotion of assembly at the microtubule plus-end. At a molar ratio corresponding to only 20% of saturation the assembly rates of the two ends of microtubules were found to differ by as much as 19-fold in the presence of XMAP whereas the ratio of assembly rates for tubulin alone is typically only 2–3 (plus/minus, see above and Mitchison and Kirschner, 1984*b*). The plus-end-specific promotion of assembly exhibited by XMAP is in contrast to mammalian τ-protein which promotes assembly of both microtubule ends equally. These observations suggest that other MAPs identified in brain and cultured cells should be examined for end specific effects on assembly.

The acceleration of plus-end microtubule assembly by XMAP is a result of both an increase in the on-rate constant of tubulin addition and a decrease in the off-rate constant. At a molar ratio of 0.012 mol XMAP/mol tubulin the rate constant for tubulin addition to the plus-end increases 10-fold (from 1.4 $s^{-1}\cdot\mu M^{-1}$ in the absence of XMAP to 15 $s^{-1}\cdot\mu M^{-1}$). At 0.01 mol XMAP/mol tubulin the plus-end off-rate decreases 10-fold from 340 s^{-1} (in the absence of XMAP) to 34 s^{-1}.

The specificity of XMAP for the microtubule plus-end and its observed effects on both the tubulin on- and off-rates at the plus-end are consistent with the assembly characteristics of microtubules in cytoplasmic extracts prepared from *Xenopus* eggs (preceding article). This correspondence further suggests that XMAP represents the major microtubule assembly factor in eggs.

The observed effects of XMAP on microtubule assembly put severe constraints on models proposed for its mechanism of action; any model constructed must account for both plus-end specificity and the observed increase in the tubulin on-rate constant promoted by XMAP. It is likely that XMAP, like the MAPs identified in vertebrate brain (Cleveland et al., 1977; Kim et al., 1979), binds along the entire microtubule

length. Although such a model in its simplest form can explain the observed decrease in the tubulin off-rate at the plus-end, greater complexity is required to explain the end-specificity (binding along the entire length of the microtubule would be expected to affect the minus-end off-rate as well) and the dramatic increase in the tubulin on-rate. It is also possible that XMAP interacts with tubulin subunits in solution, resulting in the addition of tubulin-XMAP oligomers, which might be constrained to add at the plus-end. Finally, XMAP may have a more sophisticated effect on the coupling of assembly to GTP hydrolysis that would enable it to independently influence on and off transitions at the microtubule ends. All of these models make predictions regarding the interaction of XMAP with tubulin in solution or the effect of XMAP on assembly kinetics at the minus-end. Testing of these alternative mechanisms will require measurement of the on- and off-rate of tubulin at the microtubule minus-end in the presence and absence of XMAP as well as the transition rate between growing and shrinking phases of microtubule assembly (Mitchison and Kirschner, 1984*b*).

Our use of centrosomes and flagellar axonemes as microtubule nucleation centers precludes drawing any conclusion regarding the effect of XMAP on microtubule nucleation, or on free microtubules. These aspects of XMAP function clearly need further study. In some regards the effects of XMAP on microtubule elongation might be considered a more physiological criterion for a factor responsible for temporally regulating microtubule assembly, in that most cellular microtubules are nucleated from organizing centers such as centrosomes (Brinkley et al., 1976).

Because XMAP seems to be the major activity responsible for promoting tubulin assembly in the egg, it represents a good target for regulating microtubule assembly during the cell cycle. However, XMAP is present in equal amounts in oocytes, unfertilized eggs, and cleaving eggs (unpublished observations). Thus changes in XMAP concentration (by synthesis or degradation) cannot be responsible for the observed regulation of microtubule assembly.

In this regard, it is interesting that XMAP is a phosphoprotein whose level of phosphorylation is regulated during the cell cycle. Phosphorylation of XMAP was observed to be greatest in metaphase of both meiotic and mitotic cell cycles, corresponding in phase to the observed cycle of MPF during *Xenopus* oogenesis (Gerhart et al., 1984). The modulation of XMAP phosphorylation during the cell cycle provides a possible mechanism for regulating XMAP function that should be testable in the future. XMAP is purified from eggs in interphase (15 min after activation) at a time when XMAP should be in a less phosphorylated form. The cytoplasm of such eggs is in a state favoring microtubule assembly from centrosomes as assayed in vitro (see preceding article), in vivo by measurement of microtubule polymer levels (Elinson, 1985), or by microinjection of centrosomes into activated eggs (Karsenti et al., 1984). We hypothesize that XMAP promotes assembly of interphase microtubules when it is in the dephosphorylated form. In mitosis phosphorylation of XMAP could lead to a general decrease in microtubule assembly as has been observed in fertilized *Xenopus* eggs by Elinson (1985). Establishment of the actual levels of phosphorylation of XMAP on a molar basis in interphase and metaphase (both meiotic and mitotic), and comparison of assembly-promoting activity in vitro of phosphorylated and dephosphorylated XMAP should test this hypothesis.

Note that XMAP is present in a dephosphorylated state in *Xenopus* oocytes, but that few microtubules are apparent in intact oocytes (Heidemann and Gallas, 1980; Heidemann et al., 1985) and oocyte cytoplasm is incapable of microtubule assembly in vitro (preceding article). This anomaly is explained by the presence of an inhibitor of microtubule assembly in oocyte cytoplasm (see preceding article). This inhibitor also exhibits a preference for the plus-end of microtubules. This inhibition might serve to override the microtubule assembly induced by XMAP. Indeed, preliminary evidence suggests that oocyte cytoplasm when depleted of the inhibitor (by DEAE chromatography), is capable of promoting assembly of brain tubulin (unpublished observations), presumably owing to the presence of XMAP.

In summary, we have isolated a factor from *Xenopus* eggs that dramatically promotes elongation of microtubule plus-ends. This factor, termed XMAP, is a protein of 215-kD molecular mass. XMAP acts by altering both the tubulin on- and off-rates at the plus-end. The 215-kD protein is specifically phosphorylated in M-phase, suggesting that phosphorylation regulates its activity, and thereby regulates microtubule assembly during the cell cycle of the Xenopus egg.

We thank the members of the lab for critically reading the manuscript, and Cynthia Hernandez for assisting in its preparation. We thank Gary Ward for supplying MPF, and David Drubin for τ-protein. David Kristofferson provided valuable assistance with the computer software and data analysis.

This study was supported by grants from the National Institute of General Medical Sciences and the American Cancer Society. Dr. Gard was a senior fellow of the American Cancer Society (California Division).

Received for publication 12 April 1987, and in revised form 29 June 1987.

References

Allen, C., and G. Borisy. Structural polarity and directional growth of Chlamydomonas flagella. *J. Mol. Biol.* 90:381–402.

Bloom, G. S., F. C. Luca, and R. B. Vallee. 1984. Widespread cellular distribution of MAP1A (microtubule-associated protein 1A) in the mitotic spindle and on interphase microtubules. *J. Cell Biol.* 98:331–340.

Blose, S. H., D. I. Meltzer, and J. Feramisco. 1984. 10 nm filaments are induced to collapse in living cells microinjected with monoclonal and polyclonal antibodies against tubulin. *J. Cell Biol.* 98:847–858.

Bradford, M. 1976. A rapid and sensitive method for the quantitation of microgram quantities of protein utilizing the principles of protein-dye binding. *Anal. Biochem.* 72:248–254.

Brinkley, B., G. Fuller, and D. Highland. 1976. Tubulin antibodies as probes for microtubules in dividing and non-dividing mammalian cells. *In* Cell Motility. R. Goldman, T. Pollard, and J. Rosenbaum, editor. Cold Spring Harbor Laboratory, Cold Spring Harbor, NY. 435–456.

Bulinski, J., and G. G. Borisy. 1979. Self assembly of microtubules in extracts of cultured HeLa cells and the identification of HeLa microtubule associated proteins. *Proc. Natl. Acad. Sci. USA.* 76:293–297.

Cleveland, D. W., S.-Y. Hwo, and M. W. Kirschner. 1977. Purification of tau, a microtubule-associated protein that induces assembly of microtubules from purified tubulin. *J. Mol. Biol.* 116:207–225.

Connolly, J., V. Kalnins, D. Cleveland, and M. Kirschner. 1977. Immunofluorescence staining of cytoplasmic and spindle microtubules in mouse fibroblasts with antibody to tau protein. *Proc. Natl. Acad. Sci. USA.* 74: 2437–2440.

Connolly, J. A., V. I. Kalnins, D. W. Cleveland, and M. W. Kirschner. 1978. Intracellular localization of the high molecular weight microtubule accessory protein by indirect immunofluorescence. *J. Cell Biol.* 76:781–786.

Duerr, A., D. Pallas, and F. Solomon. 1981. Molecular analysis of cytoplasmic microtubules in situ: identification of both widespread and specific proteins. *Cell.* 24:203–211.

Drubin, D. G., and M. W. Kirschner. 1986. Tau protein function in living cells. *J. Cell Biol.* 103:2739–2746.

Drubin, D., S. Kobayashi, and M. Kirschner. 1986. Association of tau protein with microtubules in living cells. *Ann. N.Y. Acad. Sci.* 466:257–268.

Elinson, R. 1985. Changes in levels of polymeric tubulin associated with activation and dorsoventral polarization of the frog egg. *Dev. Biol.* 109:224–233.

Gard, D. L., and M. W. Kirschner. 1985. A polymer-dependent increase in phosphorylation of β-tubulin accompanies differentiation of a mouse neuroblastoma cell line. *J. Cell Biol.* 100:764–774.

Gard, D. L., and M. W. Kirschner. 1987. Microtubule assembly in cytoplasmic extracts of Xenopus oocytes and eggs. *J. Cell Biol.* 105:000–000.

Gerhart, J., M. Wu, and M. Kirschner. 1984. Cell cycle dynamics of an M-phase-specific cytoplasmic factor in *Xenopus laevis* oocytes and eggs. *J. Cell Biol.* 98:1247–1255.

Heidemann, S., and P. Gallas. 1980. The effect of taxol on living eggs of *Xenopus laevis*. *Dev. Biol.* 80:489–494.

Heidemann, S., M. Hamborg, J. Balasz, and S. Lindley. 1985. Microtubules in immature oocytes of *Xenopus laevis*. *J. Cell Sci.* 77:129–141.

Herzog, W., and K. Weber. 1978. Fractionation of brain microtubule-associated proteins. *Eur. J. Biochem.* 92:1–8.

Izant, J. G., and J. R. McIntosh. 1980. Microtubule-associated proteins: a monoclonal antibody to brain microtubule associated protein 2 binds to differentiated neurons. *Proc. Natl. Acad. Sci. USA.* 77:4741–4745.

Jessus, C., C. Thibier, and R. Ozon. 1985. Identification of microtubule associated proteins (MAPs) in *Xenopus* oocyte. FEBS (Fed. Eur. Biochem. Soc.) *Lett.* 192:135–140.

Karsenti, E., R. Bravo, and M. Kirschner. 1987. Phosphorylation changes associated with the early cell cycle in *Xenopus* eggs. *Dev. Biol.* 199:442–453.

Karsenti, E., J. Newport, R. Hubble, and M. Kirschner. 1984. Interconversion of metaphase and interphase microtubule assays, as studied by injection of centrosomes and nuclei into *Xenopus* eggs. *J. Cell Biol.* 98:1730–1745.

Kim, H., L. I. Binder, and J. L. Rosenbaum. 1979. The periodic association of microtubule-associated proteins with brain microtubules in vitro. *J. Cell Biol.* 80:266–276.

Laemmli, U. 1970. Cleavage of structural proteins during the assembly of the head of bacteriophage T4. *Nature (Lond.)* 24:580–585.

Maller, J., M. Wu, and J. Gerhart. 1977. Changes in protein phosphorylation accompanying maturation of *Xenopus laevis* oocytes. *Dev. Biol.* 58:295–312.

Manes, M., and F. Barbieri. 1977. On the possibility of sperm aster involvement in dorso-ventral polarization and pronuclear migration in the amphibian egg. *J. Embryol. Exp. Morphol.* 40:187–197.

Miake-Lye, R., J. Newport, and M. Kirschner. 1983. Maturation promoting factor induces nuclear envelope breakdown in cycloheximide-arrested embryos of *Xenopus laevis*. *J. Cell Biol.* 97:81–91.

Mitchison, T., and M. Kirschner. 1984*a*. Microtubule assembly nucleated by isolated centrosomes. *Nature (Lond.)* 312:232–237.

Mitchison, T., and M. Kirschner. 1984*b*. Dynamic instability of microtubule growth. *Nature* 312:237–242.

Newport, J., and M. Kirschner. 1982. A major developmental transition in early *Xenopus* embryos. I. Characterization and timing of cellular changes at the midblastula stage. *Cell.* 30:675–686.

Olmsted, J. 1986. Microtubule-associated proteins. *Annu. Rev. Cell Biol.* 2:421–457.

Stewart-Savage, J., and R. D. Grey. 1982. The temporal and spatial relationships between cortical contraction, sperm trail formation, and pronuclear migration in fertilized eggs of *Xenopus laevis*. *Wilhelm Roux's Arch. Dev. Biol.* 191:241–245.

Vallee, R. B. 1982. A taxol-dependent procedure for the isolation of microtubules and microtubule associated proteins (MAPs). *J. Cell Biol.* 92:435–422.

Vallee, R. B., and G. S. Bloom. 1983. Isolation of sea urchin egg microtubules with taxol and identification of mitotic spindle microtubule associated proteins with monoclonal antibodies. *Proc. Natl. Acad. Sci. USA.* 80:6259–6263.

Wu, M., and Gerhart, J. 1980. Partial purification and characterization of the maturation promoting factor from eggs of *Xenopus laevis*. *Dev. Biol.* 79: 465–477.